Characterization of SSMVEP-based EEG signals using multiplex limited penetrable horizontal visibility graph

Cite as: Chaos **29**, 073119 (2019); https://doi.org/10.1063/1.5108606
Submitted: 30 April 2019 . Accepted: 09 July 2019 . Published Online: 31 July 2019

Zhong-Ke Gao, Wei Guo, Qing Cai, Chao Ma, Yuan-Bo Zhang, and Jürgen Kurths

Characterization of SSMVEP-based EEG signals using multiplex limited penetrable horizontal visibility graph

Cite as: Chaos **29**, 073119 (2019); doi: 10.1063/1.5108606
Submitted: 30 April 2019 · Accepted: 9 July 2019 ·
Published Online: 31 July 2019

Zhong-Ke Gao,[1] Wei Guo,[1] Qing Cai,[1] Chao Ma,[1,a)] Yuan-Bo Zhang,[2] and Jürgen Kurths[3,4]

AFFILIATIONS

[1]School of Electrical and Information Engineering, Tianjin University, Tianjin 300072, China
[2]School of Civil Engineering, Tianjin University, Tianjin 300072, China
[3]Potsdam Institute for Climate Impact Research, Telegraphenberg A31, 14473 Potsdam, Germany
[4]Department of Physics, Humboldt University Berlin, 12489 Berlin, Germany

Note: The paper is part of the Focus Issue, "Complex Network Approaches to Cyber-Physical Systems."
[a)]**Electronic mail:** chao.ma@tju.edu.cn

ABSTRACT

The steady state motion visual evoked potential (SSMVEP)-based brain computer interface (BCI), which incorporates the motion perception capabilities of the human visual system to alleviate the negative effects caused by strong visual stimulation from steady-state VEP, has attracted a great deal of attention. In this paper, we design a SSMVEP-based experiment by Newton's ring paradigm. Then, we use the canonical correlation analysis and Support Vector Machines to classify SSMVEP signals for the SSMVEP-based electroencephalography (EEG) signal detection. We find that the classification accuracy of different subjects under fatigue state is much lower than that in the normal state. To probe into this, we develop a multiplex limited penetrable horizontal visibility graph method, which enables to infer a brain network from 62-channel EEG signals. Subsequently, we analyze the variation of the average weighted clustering coefficient and the weighted global efficiency corresponding to these two brain states and find that both network measures are lower under fatigue state. The results suggest that the associations and information transfer efficiency among different brain regions become weaker when the brain state changes from normal to fatigue, which provide new insights into the explanations for the reduced classification accuracy. The promising classification results and the findings render the proposed methods particularly useful for analyzing EEG recordings from SSMVEP-based BCI system.

A brain-computer interface (BCI) allows a human brain to interact with an external device and empowers individuals who have trouble interacting mechanically with the world. The steady-state motion visual evoked potentials (SSMVEPs), which are used in brain computer interface (BCI)-based systems, have an advantage of alleviating the negative effects on the brain system. We here use the traditional canonical correlation analysis (CCA) and Support Vector Machines (SVM) to classify the collected SSMVEP-based EEG signals. As an unavoidable problem, the mental fatigue state that occurs after a long time use of the BCI-based system directly affects the efficiency of the BCI system. Without a high classification accuracy, users cannot control external devices accurately. Investigating fatigue behavior from the perspective of brain network may contribute to the improvement of classification accuracy under fatigue state. Therefore, we develop a multiplex limited penetrable horizontal visibility graph (MLPHVG) method to characterize normal and fatigued behavior. The results indicate that our method allows probing into the fatigued behavior resulting from a long duration of SSMVEP-based BCI systems.

I. INTRODUCTION

The brain computer interface (BCI), also known as brain machine interface (BMI), is a system that allows a human brain to interact directly with the surrounding environment using electroencephalography (EEG) as a control signal.[1] Over the past few decades, EEG-based BCI analysis has attracted more and more attention. Neuper *et al.*[2] proposed an EEG-based BCI to train a completely paralyzed patient with severe cerebral palsy for verbal communication.

Lopez-Gordo *et al.*[3] presented a novel fully auditory EEG-BCI system that could provide a clinically useful communication to the visually problematic user. Moctezuma *et al.*[4] evaluated the feasibility of the EEG-recorded imagined speech for subject identification. Ang *et al.*[5] investigated the efficacy of an EEG-based MI BCI system coupled with MIT-Manus shoulder-elbow robotic feedback (BCI-Manus) for subjects with chronic stroke with upper-limb hemiparesis.

A large number of studies have demonstrated that the EEG signals stimulated by experimental paradigms can be used as control signals for BCI systems. Common adopted paradigms include visual evoked potentials (VEPs),[6] slow cortical potentials (CSPs),[7] P300 evoked potentials,[8] Motor Imagery (MI),[9] and sensorimotor rhythms (SRs).[10] Among them, VEPs are the brain regulating activities that occur in the visual cortex when visual stimuli appear, and these modulations are relatively easy to detect.[11] According to the stimulation frequency, VEPs can be divided into transient VEP (TVEP)[12] and steady-state VEP (SSVEP).[13] Compared with TVEP, SSVEP has a higher information transfer rate, more stable signal quality, simpler system configuration, and shorter training time. In addition, SSVEP is less affected by eye movements and other noises, which makes it more commonly used in BCI system.[1] In recent years, many SSVEP paradigms based on changes in flicker or contrast have been proposed.[14–16] However, a long-term flickering of visual stimulator can easily lead to visual and mental fatigue, which in turn reduces the accuracy of BCI systems.[17] Fortunately, researchers have developed steady state motion visual evoked potential (SSMVEP)-based BCI systems to mitigate this negative impact.[18–20] The SSMVEP is a periodic response to a visual stimulus modulated, although there is some loss in classification accuracy, it has effectively improved the discomfort caused by long-term use of the BCI system.

Recently, the complex network theory has been applied to analysis of complex systems. In particular, time series analysis using the complex network theory have achieved fruitful results in interdisciplinary fields,[21–29] such as multiphase flow,[30–32] brain function,[33–35] and climatic networks.[36,37] Brain, as the control center of the nervous system, is a complex system composed of a mass of neurons.[38] The underlying mechanisms of brain are still elusive and remain a challenging problem. Complex network provides a new way to characterize changes in the function and behavior of brain networks from EEG.[39–41] Kong *et al.*[42] analyzed the different mental states of drivers and found a neurometric measure that can detect driver fatigue. Supriya *et al.*[43] used a weighted visibility graph to analyze epileptic EEG signals. However, few people have applied the complex network method to explore changes of the brain function network in the SSMVEP-based experiment, especially how the brain function network changes after a long time of operation. The visibility graph (VG) theory, which has been proved to be an efficient method, allows to characterize complex systems from time series. Lacasa *et al.*[44,45] proposed the horizontal visibility graph (HVG) and the multiplex visibility graph (MVG), which allow mapping a time series into a complex network. The limited penetrable visibility graph (LPVG)[46] method, that can effectively filter out noise interference, has been successfully applied to the analysis of univariate time series. But the applicability of the visibility graph methods has been limited to the study of univariate time series to a large extent. Recently, we have developed a novel Multiplex Limited Penetrable Horizontal Visibility Graph (MLPHVG) method, which allows analyzing multivariate EEG signals.[47] In this study, we further develop the MLPHVG method to characterize the fatigue and normal brain behavior underlying SSMVEP-based EEG signals.

In this paper, we first design a SSMVEP-based experiment to explore the fatigued brain behavior. We use the canonical correlation analysis (CCA) and Support Vector Machines (SVMs) to probe the influence of fatigue on the SSMVEP classification accuracy. During the experiment, we find that a long-term continuous operation can cause unavoidable fatigue problems, thus reducing classification accuracy. Hence, it is necessary to seek for an efficient method to explain the brain behavior under fatigue state to reveal this difference. In this study, a MLPHVG method is applied to analyze the EEG signals generated by the SSMVEP stimulation paradigm. The results indicate that our methods enable to greatly improve the classification accuracy of SSMVEP-based EEG signals and allow characterizing the difference of the brain network process between normal and fatigue states.

II. EXPERIMENTAL SETUP

A. Experimental environment

In our experiment, EEG data are acquired by a Neuroscan EEG system (SynAmps2) with a sampling frequency of 1 kHz. A 64-channel EEG cap is used to collect EEG signals with electrodes assigned according to the "International 10–20 electrodes position system" method.[48] The locations of the electrodes are shown in Fig. 1.

The visual stimulator refers to the Newton's ring paradigm,[19] which is controlled by the Psychophysics Toolbox 3.0[49] and presented on a 24-in. LCD screen with a screen refresh rate of 60 Hz. Newton's ring motion stimulation is composed of the same black and white ring of 4 groups of centers. Actually, repetitive visual stimuli with a low frequency (6–15 Hz) have been widely used in high performance BCI systems due to their strong response.[50] However, the steady state method has certain limitations, especially due to the disappearance of the response signal caused by the further superposition of the signal.[51] Therefore, we select some frequencies in low and medium frequency bands[52] (6 Hz, 8 Hz, 10 Hz, 12 Hz, 14 Hz, 16 Hz, 18 Hz, 20 Hz) as the stimulation frequency of 8 stimulators. In fact, each of these 8 stimulation frequencies can induce a corresponded EEG signal, which can be used as a control signal for controlling external devices. The visual stimulator of the SSMVEP experiment and its corresponding flicker frequency and image size parameters are shown in Fig. 2.

B. Participants and experimental procedure

10 healthy adults (5 males, 5 females, ages 22–25) are recruited in the experiment, who are right-handed, with a normal or corrected to normal visual acuity, no history of brain diseases, and have lunch break habits. Prior to the experiment, the reference electrodes M1 and M2 are placed at the mastoids of the left and right ears of the subject, REF is placed at the top zone, and the ground electrode FPZ is placed at the forehead. The electrode impedance of all channels is below 5 KΩ.

All experiments are carried out in a quiet room, and the subject sit relaxed on a chair with a field of view approximately 70 cm from the center of the visual stimulator. Each SSMVEP-based experiment

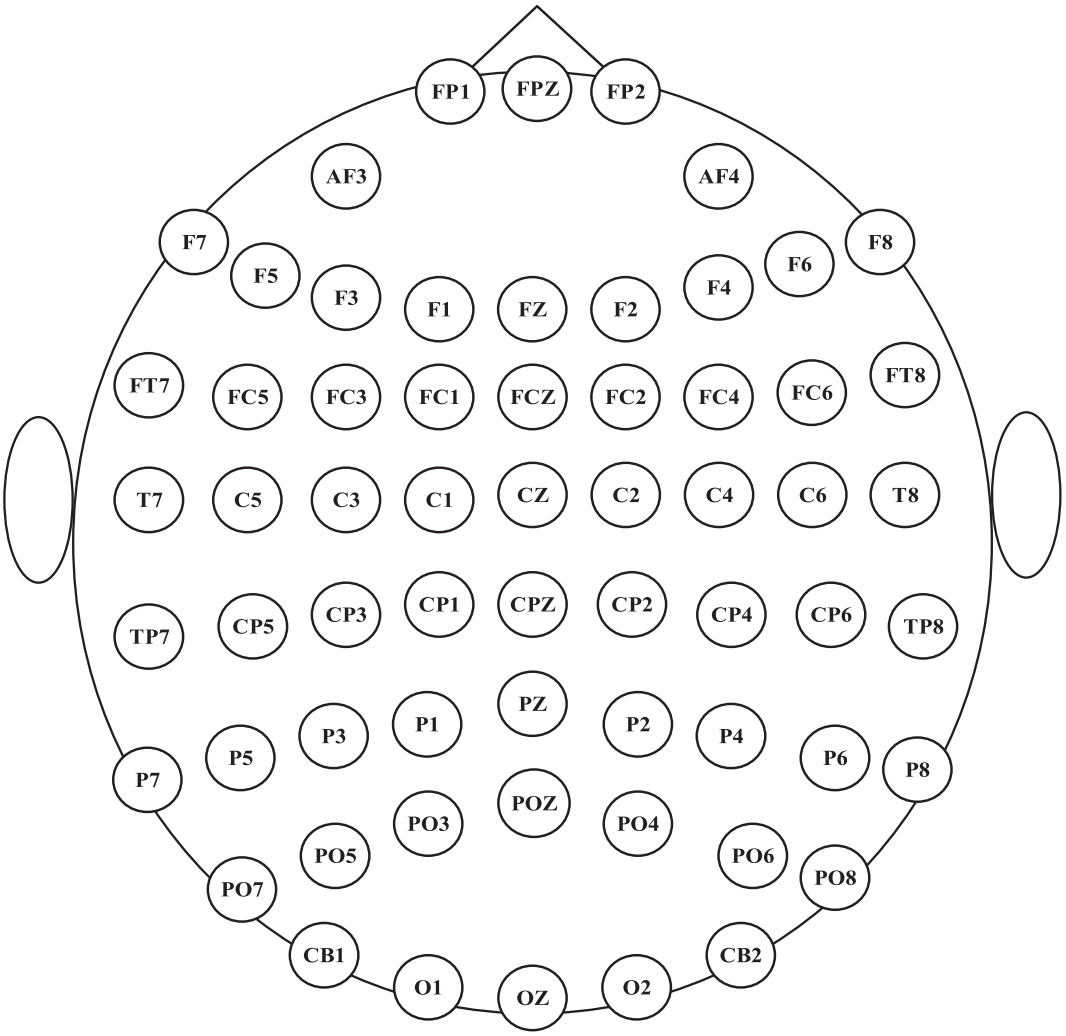

FIG. 1. Electrode locations.

lasts for about 36 min, which consists of 3 sessions, and there is a 4 min break after each session. Before the experiment, eight stimulus targets (Newton's ring paradigms) will be presented simultaneously on the LCD screen at different oscillation frequencies in a fixed order. When the experiment starts, a digital sound prompt will appear to remind the subject to start the experiment and to increase the attention. During each session, eight stimulus targets are placed in the order of the frequency from small to large and corresponded to the sound prompts from 1 to 8. For each session, subjects need to steer his (her) eyes on the stimulus target of the corresponding number for 4 s when hearing the sound prompts, one by one during a trial. Then, an end sound will prompt the subject to have a 2 s break away from the stimulation interface, while waiting for the next sound prompt to arrive. In this way, traversing 8 different frequency visual stimulators in the order from 1 to 8 is called a trial, and one session includes 10 trials.

During the whole experiment, the subjects are required to keep quiet, focus on watching the excitation interface, and try to avoid a rapid motion of the head. Before and after each session, all participants need to fill out a fatigue status questionnaire which contains 5 dimensions and 20-item self-report instrument. The score of each dimension reflects the severity of fatigue, the higher the score, the more severe the fatigue. We use the Multidimensional Fatigue Inventory (MFI)[53] to estimate the score of each participant to measure their fatigue level. The subjects take the experiments in normal and fatigue state. Each experiment consists of 3 sessions, so there are 6 sessions for each subject. The structure of the BCI system is given in Fig. 3.

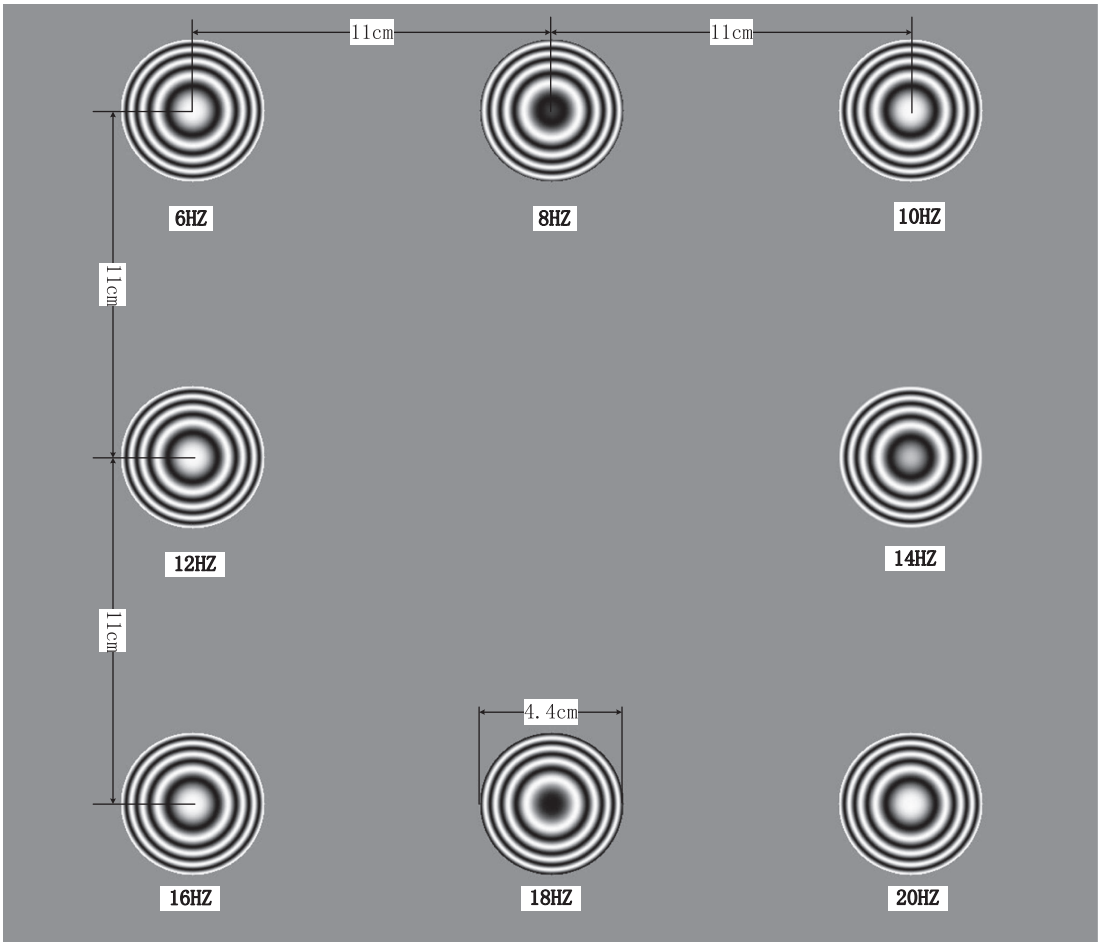

FIG. 2. The user interface shown to the subjects and corresponding parameters to the visual stimulator of the experiment.

C. Experiment data processing

All acquired 62-channel EEG data are preprocessed by using EEGLAB.[54] A band-pass filtering of 1–40 Hz is performed for filtering the EEG signals. A 50 Hz notch filter is applied to the EEG data to eliminate AC power supply noise. Finally, noise and EOG (electric eye) artifacts are removed by using the Independent Component Analysis (ICA).[55] After that, there are 62 channels for the preprocessed EEG signals.

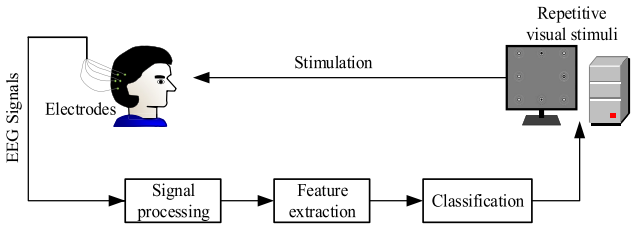

FIG. 3. The structure of the SSMVEP-based BCI system.

III. CLASSIFICATION OF SSMVEP SIGNAL

We select O1, OZ, O2, PO3, PO4, PO7, PO8, and POZ for classification calculation. These 8 EEG channels are in the occipital region and parietal occipital region, which have commonly been selected for SSVEP-based BCI studies.[56,57]

We apply the canonical correlation analysis (CCA)[58] to extract features from the processed data. CCA is a multivariate statistical analysis method, which can be used to extract a linear combination of data with the greatest correlation. Also, CCA has a wide range of applications in frequency analysis under the SSVEP paradigm.[59] Here, we analyze the preprocessed data as a set of variables, the reference signal comprised of sine-cosine waves at the stimulus frequency, and use CCA to calculate their correlation.

Specifically, we define a group of variables as X,

$$X = \begin{bmatrix} channel(1) \\ channel(2) \\ \vdots \\ channel(8) \end{bmatrix}, \tag{1}$$

where X contains 8 channels of EEG signals, each channel contains data of 4 s length.

The reference signal is defined as Y,

$$Y = \begin{bmatrix} \sin(2\pi f_1 t) \\ \cos(2\pi f_1 t) \\ \vdots \\ \sin(2\pi f_8 t) \\ \cos(2\pi f_8 t) \end{bmatrix}. \tag{2}$$

In this paper, we do not consider harmonic components. $f_1 \sim f_8$ are 6 Hz, 8 Hz, 10 Hz, 12 Hz, 14 Hz,16 Hz, 18 Hz and 20 Hz, respectively. Each signal in Y has the same length as signal in X.

CCA seeks two weight vectors, W_x and W_y, by maximizing the correlation coefficient $\rho(x, y)$ between $x = W_x^T X$ and $y = W_y^T Y$. That is, W_x and W_y can be obtained by maximizing the following functions:

$$\begin{aligned} \max_{W_x, W_y} \rho(x, y) &= \frac{E[x^T y]}{\sqrt{E[x^T x] \cdot E[y^T y]}} \\ &= \frac{E[W_x^T X Y^T W_y]}{\sqrt{E[W_x^T X X^T W_x] \cdot E[W_y^T Y Y^T W_y]}}, \\ &= \frac{W_x^T E[X Y^T] W_y}{\sqrt{W_x^T E[X X^T] W_x \cdot W_y^T E[Y Y^T] W_y}} \\ &= \frac{W_x^T C_{xy} W_y}{\sqrt{W_x^T C_{xx} W_x \cdot W_y^T C_{yy} W_y}}, \end{aligned} \tag{3}$$

where E is the sample expectation, C_{xy} is the cross covariance matrix between X and Y, C_{xx} and C_{yy} represent the covariance matrices of X and Y, respectively.

Via setting SSMVEP signals as X, we can utilize CCA to get one-dimensional variable $x = W_x^T X$. Then, the fast Fourier transform (FFT) is applied to calculate x and the spectrum energy sequence u_f is obtained,

$$u_f = |FFT(x)|. \tag{4}$$

Then, we extract the spectral energy u_f at 8 stimulation frequency points $f_1 \sim f_8$ to build the feature vector P,

$$P = [u_{f_1}, u_{f_2}, u_{f_3}, u_{f_4}, u_{f_5}, u_{f_6}, u_{f_7}, u_{f_8}]. \tag{5}$$

Support Vector Machine (SVM),[60,61] as a supervised learning method, is ideal for analyzing multichannel EEG signals because of its good generalization capability. It separates the two categories of samples by constructing a hyperplane, which minimizes the empirical classification error and the geometric margin in the classification task. Here, we feed above-obtained feature vector into SVM to classify the SSMVEP signals. For each subject, we calculate the classification accuracy of EEG signals recorded under normal and fatigue states, respectively. The results obtained by CCA + SVM algorithm for each subject under two mental states are shown in Fig. 4. We find that the CCA + SVM performs well in the SSMVEP classification. The results demonstrated that the mental fatigue states can lead to a decrease in SSMVEP classification accuracy. In addition, we calculate the average accuracy of 10 subjects under the two mental states, respectively. In the normal states, the average classification accuracy is 87.88%, while it decreases to 68.31% in the mental fatigue states. The decreased classification accuracy caused by fatigue will directly affect the control performance of the SSMVEP-based BCI system. Therefore, we probe into the fatigue mechanism in terms of the brain network analysis by using the MLPHVG method in Sec. IV.

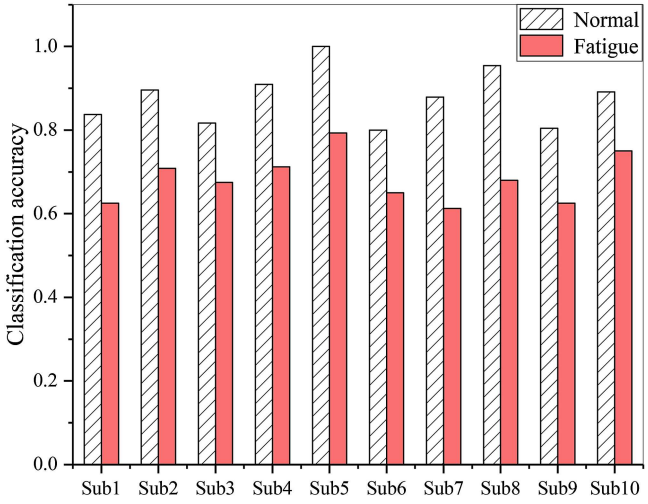

FIG. 4. Classification accuracy in brain states of normal and mental fatigue.

IV. CHARACTERIZING FATIGUE BEHAVIOR VIA MULTILAYER COMPLEX NETWORKS

For each subject participating in the experiment, we collect two types of mental states within the 320 s experiment under the SSMVEP stimulation paradigm: normal state and fatigue state. Then, we divide each EEG signal into 4 s non-overlapped segments (80 EEG segments are obtained). We then randomly select 20 EEG segments for the subsequent complex network analysis.

A. Methodology

For univariate time series $\{x_i\}_{i=1}^N$ of length N, the corresponding Limited Penetrable Horizontal Visibility Graph (LPHVG) can be constructed as follows:

(1) Vertical bars are constructed for the univariate time series, and the height of the straight column is in accordance with each time point as shown in Fig. 5(a); (2) for any paired nodes a and b, when the horizontal connection between the two straight columns does not intersect any of the straight columns between the nodes, then a connection between these two nodes is set [black lines in Fig. 5(b)]; (3) if

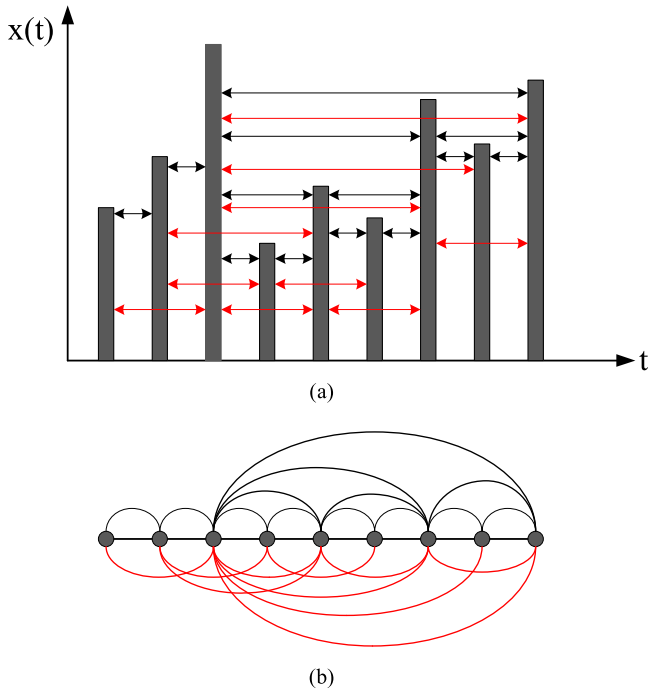

FIG. 5. (a) A time series and (b) its corresponding LPHVG with the limited penetrable distance being 1.

we define the limited penetrable distance to L, a connection between two nodes exists if the number of in-between nodes that block the horizontal connection does not exceed L [red lines in Fig. 5(b)].

For a multivariate time series $\{x_{\alpha,i}\}_{i=1}^{N}$, $\alpha = 1, 2, \ldots, M$, containing M channels of EEG signals of equal length N, a LPHVG can be constructed for each EEG signal with penetrable distance $L = 1$. Then, we obtain an M-layer complex network $\{A^{\alpha}\}_{\alpha=1}^{M}$, where we define each layer of the network as a node, then we calculate an interlayer correlation between layers α and β as the functional connectivity as follows:

$$I_{\alpha,\beta} = \sum_{k^{\alpha}} \sum_{k^{\beta}} p(k^{\alpha}, k^{\beta}) \log \frac{p(k^{\alpha}, k^{\beta})}{p(k^{\alpha}) p(k^{\beta})}, \tag{6}$$

where $p(k^{\alpha})$ is a probability that a node has a degree of k^{α} at layer α, which can be used to express the degree distribution of the α-th layer. The degree of the node i in the layer α network is expressed as k_i^{α},

$$k_i^{\alpha} = \sum_{j=1}^{N} a_{ij}^{\alpha}. \tag{7}$$

The joint probability of finding a node having degree equal to k^{α} and k^{β}, respectively, at layer α and at layer β can be computed by

$$p(k^{\alpha}, k^{\beta}) = \frac{N_{k^{\alpha}, k^{\beta}}}{N}, \tag{8}$$

where $N_{k^{\alpha},\, k^{\beta}}$ is the number of nodes having degree equal to k^{α} and k^{β} in layer α and layer β, respectively.

We then construct a brain network by regarding each layer as a node and determining the functional connectivity by calculating the interlayer correlation of all paired layers. In this paper, we apply a MLPHVG method to perform a SSMVEP-based fatigue investigation using the 62-channel EEG data collected in our experiment. The three main steps of the method are shown in Fig. 6.[62]

B. Charactering fatigue behavior from EEG signals

The brain networks corresponding to normal and fatigue states can be derived from MLPHVGs. The generated brain network is a fully-connected weighted network with 62 nodes. The integrals of the network measures over the sparsity range (corresponding to the areas of the network measure curve within the sparsity range) are taken into account. For each generated brain network, a wide range of sparsity ($10\% \leq S \leq 35\%$) with an interval of 1% will be utilized. This way for determining the connections has been widely used in the network construction.[63] Sparsity (S) is defined as the ratio of the number of existing edges to the maximum possible edge number in the network. Then, we calculate the average weighted clustering coefficient (C^w) and the weighted global efficiency (E_{glo}^w) to investigate the topology of the brain network.[64] The network measures can be calculated as follows:

$$\begin{cases} C^w = \dfrac{\sum_{i \in N} C_i^w}{n}, \\ C_i^w = \dfrac{\sum_{j,l \neq i \in N} (w_{ij} w_{lj} w_{il})^{1/3}}{k_i (k_i - 1)}, \end{cases} \tag{9}$$

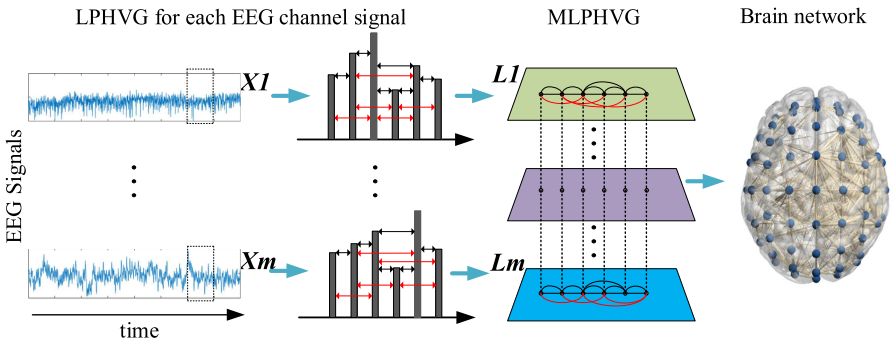

FIG. 6. The MLPHVG method construction process.

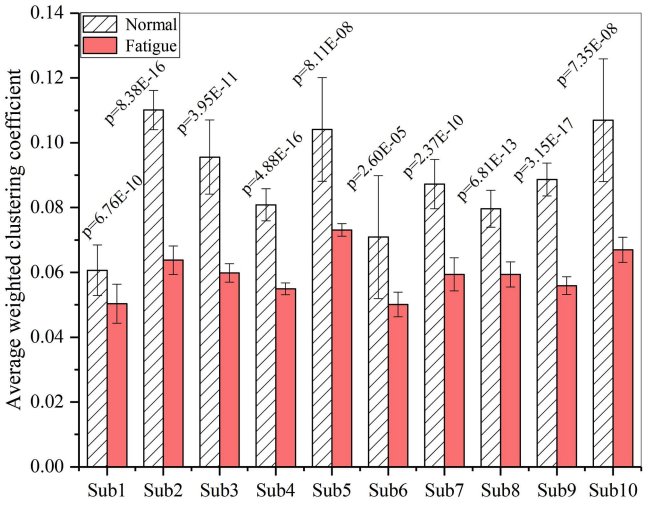

FIG. 7. The average weighted clustering coefficient under normal and mental fatigue states for different subjects.

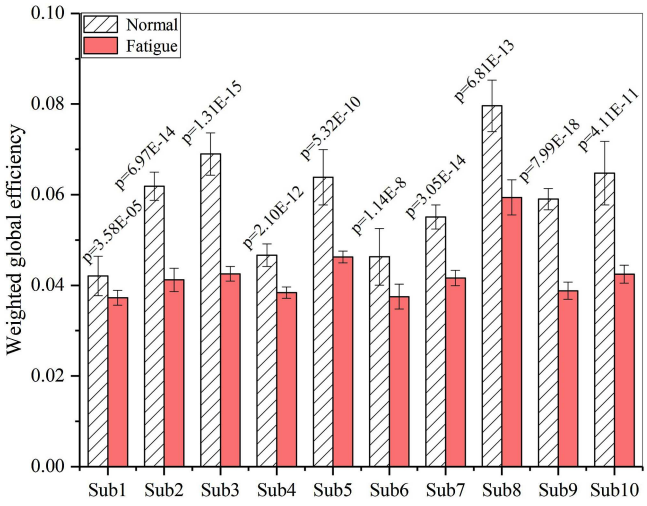

FIG. 8. The weighted global efficiency under normal and mental fatigue states for different subjects.

$$E_{glo}^{w} = \frac{1}{N(N-1)} \sum_{i \neq j \in N} (d_{ij})^{-1}, \tag{10}$$

where N is the set of all nodes in the network; n is the number of nodes; C_i^w is the average weighted clustering coefficient of nodes i; k_i is the degree of node i; w_{ij}, w_{il}, and w_{lj} represent the weight between node i and j, i and l, l and j, respectively; d_{ij} is the shortest weighted path length between nodes i and j.

For each subject participating in the experiment, we collect 20 sets of multichannel EEG signal samples in the normal state and 20 sets of multichannel EEG samples in the fatigue state and construct the MLPHVGs network for each sample. Then, the average weighted clustering coefficient and the weighted global efficiency are calculated for each epoch and the average results for each subject are shown in Figs. 7 and 8. In addition, the *t-test* is employed to evaluate the p-value of the network measurements between normal and fatigue states. We find that there is a significant difference between the two sets of samples when the p-values are much less than 0.05. From Figs. 7 and 8, we can see that the subjects under mental fatigue state have lower average weighted clustering coefficient and weighted global efficiency.

In the SSMVEP experiments, the subjects need to focus on the stimulation target to complete the cognitive work, so they will bear a greater cognitive workload under fatigue state compared with normal state. Also, their cognitive ability is consequently reduced. The average global efficiency is a measure of the global information transfer efficiency of the whole brain network. In particular, cognitive function has a connection with the global efficiency of information transfer.[65] A decreased global efficiency reflects a worse performance of cognitively effortful tasks which is associated with less integration of processing in brain networks.[66,67] Through the integrals of the network measures, we find that the weighted global efficiency decreased as the brain changes from the normal to fatigue state, indicating that the connections and tightness between the functional modules of the brain network are weakened. A weaker connection between modules of brain functional networks usually corresponds to a lower global efficiency, which may result from the fatigue state resulting from a long use of the SSMVEP-based BCI system. Zhang *et al.*[66] have indicated that fatigue has a negative impact on the network efficiency. Their results well support our interesting findings in the characterization of brain fatigue behavior from the SSMVEP-based BCI system.

V. CONCLUSION

In this study, we have designed a SSMVEP-based experiment and use the CCA + SVM algorithm to classify the SSMVEP signals in both normal and fatigue states. The results of 10 subjects show that the classification accuracy under normal states is generally higher than that under fatigue states. In order to explore the reasons for the difference in classification accuracy under normal and fatigue states, we have developed a MLPHVG-based multilayer complex network model to characterize brain behavioral changes using SSMVEP signals. Through the construction of brain networks and the analysis of network measures, we discover that each subject's average weighted clustering coefficient and global efficiency decrease under the fatigue states. This finding also suggests that the brain network presents lower global information transfer efficiency in the fatigue states during the SSMVEP experiments. The reduction in global efficiency leads to a reduction in classification accuracy, which reveals the difference in classification accuracy between normal state and fatigue state from the perspective of a brain network. Our method allows an effective characterization of the normal and fatigue behavior of brain and ensures a broad application in the SSMVEP-based BCI system.

ACKNOWLEDGMENTS

This work is supported by National Natural Science Foundation of China (NNSFC) under Grant No. 61873181.

REFERENCES

[1]J. R. Wolpaw, N. Birbaumer, W. J. Heetderks, D. J. McFarland, P. H. Peckham, G. Schalk, E. Donchin, L. A. Quatrano, C. J. Robinson, and T. M. Vaughan, "Brain-computer interface technology: A review of the first international meeting," IEEE Trans. Rehabil. Eng. **8**(2), 164–173 (2000).

[2]C. Neuper, G. R. Müller, A. Kübler, N. Birbaumer, and G. Pfurtscheller, "Clinical application of an EEG-based brain-computer interface: A case study in a patient with severe motor impairment," Clin. Neurophysiol. **114**(3), 399–409 (2003).

[3]M. A. Lopez-Gordo, E. Fernandez, S. Romero, F. Pelayo, and A. Prieto, "An auditory brain-computer interface evoked by natural speech," J. Neural Eng. **9**(3), 036013 (2012).

[4]L. A. Moctezuma, A. A. Torres-García, L. Villaseñor-Pineda, and M. Carrillo, "Subjects identification using EEG-recorded imagined speech," Expert Syst. Appl. **118**, 201–208 (2019).

[5]K. K. Ang, K. S. G. Chua, K. S. Phua, C. C. Wang, Z. Y. Chin, C. W. K. Kuah, W. Low, and C. T. Guan, "A randomized controlled trial of EEG-based motor imagery brain-computer interface robotic rehabilitation for stroke," Clin. EEG Neurosci. **46**(4), 310–320 (2015).

[6]S. Nehamkin, M. Windom, and T. U. Syed, "Visual evoked potentials," Am. J. Electroneurod. Technol. **48**(4), 233–48 (2008).

[7]N. Birbaumer, "Slow cortical potentials: Plasticity, operant control, and behavioral effects," Neuroscience **5**(2), 74–78 (1999).

[8]B. K. Bonala and B. H. Jansen, "A computational model for generation of the P300 evoked potential component," J. Integr. Neurosci. **11**(3), 277–294 (2012).

[9]G. Pfurtscheller and C. Neuper, "Motor imagery and direct brain-computer communication," IEEE Proc. **89**(7), 1123–1134 (2001).

[10]A. Kubler, F. Nijboer, J. Mellinger, T. M. Vaughan, H. Pawelzik, G. Schalk, D. J. McFarland, N. Birbaumer, and J. R. Wolpaw, "Patients with ALS can use sensorimotor rhythms to operate a brain-computer interface," Neurology **64**(10), 1775–1777 (2005).

[11]B. Bromm, "Human brain electrophysiology. Evoked potentials and evoked magnetic fields in science and medicine," Pain **39**(3), 371–372 (1989).

[12]W. G. Sannita, L. Lopez, C. Piras, and G. Di Bon, "Scalp-recorded oscillatory potentials evoked by transient pattern-reversal visual stimulation in man," Clin. Neurophysiol. **96**(3), 206–218 (1995).

[13]H. Strasburger, W. Scheidler, and I. Rentschler, "Amplitude and phase characteristics of the steady-state visual evoked potential," Appl. Opt. **27**(6), 1069–88 (1988).

[14]S. Parini, L. Maggi, A. C. Turconi, and G. Andreoni, "A robust and self-paced BCI system based on a four class SSVEP paradigm: Algorithms and protocols for a high-transfer-rate direct brain communication," Comput. Intell. Neurosci. **2009**, 864564 (2009).

[15]Z. H. Wu, Y. X. Lai, Y. Xia, D. Wu, and D. Z. Yao, "Stimulator selection in SSVEP-based BCI," Med. Eng. Phys. **30**(8), 1079–1088 (2008).

[16]D. H. Zhu, J. Bieger, G. Garcia Molina, and R. M. Aarts, "A survey of stimulation methods used in SSVEP-based BCIs," Comput. Intell. Neurosci. **2010**, 702357 (2010).

[17]S. Ajami, A. Mahnam, and V. Abootalebi, "An adaptive SSVEP-based brain-computer interface to compensate fatigue-induced decline of performance in practical application," IEEE Trans. Neural Syst. Rehabil. Eng. **26**(11), 2200–2209 (2018).

[18]B. Hong, F. Guo, T. Liu, X. R. Gao, and S. K. Gao, "N200-speller using motion-onset visual response," Clin. Neurophysiol. **120**(9), 1658–1666 (2009).

[19]J. Xie, G. H. Xu, J. Wang, F. Zhang, and Y. Z. Zhang, "Steady-state motion visual evoked potentials produced by oscillating Newton's rings: Implications for brain-computer interfaces," PLoS One **7**(6), e39707 (2012).

[20]W. Q. Yan, G. H. Xu, J. Xie, M. Li, and Z. Y. Dan, "Four novel motion paradigms based on steady-state motion visual evoked potential," IEEE T. Bio. Med. Eng. **65**(8), 1696–1704 (2018).

[21]J. Zhang and M. Small, "Complex network from pseudoperiodic time series: Topology versus dynamics," Phys. Rev. Lett. **96**(23), 238701 (2006).

[22]X. K. Xu, J. Zhang, and M. Small, "Superfamily phenomena and motifs of networks induced from time series," Proc. Natl. Acad. Sci. **105**(50), 19601–19605 (2008).

[23]J. F. Donges, R. V. Donner, M. H. Trauth, N. Marwan, H. J. Schellnhuber, and J. Kurths, "Nonlinear detection of paleoclimate-variability transitions possibly related to human evolution," Proc. Natl. Acad. Sci. **108**(51), 20422–20427 (2011).

[24]J. H. Feldhoff, R. V. Donner, J. F. Donges, N. Marwan, and J. Kurths, "Geometric detection of coupling directions by means of inter-system recurrence networks," Phys. Lett. A **376**(46), 3504–3513 (2012).

[25]R. X. Xiang, J. Zhang, X. K. Xu, and M. Small, "Multiscale characterization of recurrence-based phase space networks constructed from time series," Chaos **22**(1), 013107 (2012).

[26]Y. Zou, R. V. Donner, N. Marwan, J. F. Donges, and J. Kurths, "Complex network approaches to nonlinear time series analysis," Phys. Rep. **787**, 1–97 (2019).

[27]N. Marwan, J. F. Donges, Y. Zou, R. V. Donner, and J. Kurths, "Complex network approach for recurrence analysis of time series," Phys. Lett. A **373**(46), 4246–4254 (2009).

[28]Z. K. Gao, M. Small, and J. Kurths, "Complex network analysis of time series," Europhys. Lett. **116**(5), 50001 (2016).

[29]J. Zhang, J. F. Sun, X. D. Luo, K. Zhang, T. Nakamura, and M. Small, "Characterizing pseudoperiodic time series through the complex network approach," Physica D **237**(22), 2856–2865 (2008).

[30]W. D. Dang, Z. K. Gao, L. H. Hou, D. M. Lv, S. M. Qiu, and G. R. Chen, "A novel deep learning framework for industrial multiphase flow characterization," in IEEE Transactions on Industrial Informatics (IEEE, 2019).

[31]Z. K. Gao, S. S. Zhang, W. D. Dang, S. Li, and Q. Cai, "Multilayer network from multivariate time series for characterizing nonlinear flow behavior," Int. J. Bifurc. Chaos **27**(4), 1750059 (2017).

[32]Z. K. Gao, W. D. Dang, C. X. Mu, Y. X. Yang, S. Li, and C. Grebogi, "A novel multiplex network-based sensor information fusion model and its application to industrial multiphase flow system," IEEE Trans. Industr. Inform. **14**(9), 3982–3988 (2018).

[33]Z. K. Gao, K. L. Zhang, W. D. Dang, Y. X. Yang, Z. B. Wang, H. B. Duan, and G. R. Chen, "An adaptive optimal-kernel time-frequency representation-based complex network method for characterizing fatigued behavior using the SSVEP-based BCI system," Knowl. Based Syst. **152**, 163–171 (2018).

[34]Z. K. Gao, S. Li, Q. Cai, W. D. Dang, Y. X. Yang, C. X. Mu, and P. Hui, "Relative wavelet entropy complex network for improving EEG-based fatigue driving classication," IEEE Trans. Instrum. Meas. **68**(7), 2491–2497 (2018).

[35]Z. K. Gao, Q. Cai, Y. X. Yang, N. Dong, and S. S. Zhang, "Visibility graph from adaptive optimal kernel time-frequency representation for classification of epileptiform EEG," Int. J. Neur. Syst. **27**(4), 1750005 (2017).

[36]N. Boers, B. Goswami, A. Rheinwalt, B. Bookhagen, B. Hoskins, and J. Kurths, "Complex networks reveal global pattern of extreme-rainfall teleconnections," Nature **566**(7744), 373–377 (2019).

[37]N. Marwan and J. Kurths, "Complex network based techniques to identify extreme events and (sudden) transitions in spatio-temporal systems," Chaos **25**(9), 097609 (2015).

[38]E. Bullmore and O. Sporns, "Complex brain networks: Graph theoretical analysis of structural and functional systems," Nat. Rev. Neurosci. **10**(3), 186–98 (2009).

[39]L. Y. Cui, S. Kumara, and R. Albert, "Complex networks: An engineering view," IEEE Circ. Syst. Mag. **10**(3), 10–25 (2010).

[40]G. Yan, J. Ren, Y. C. Lai, C. H. Lai, and B. W. Li, "Controlling complex networks: How much energy is needed?," Phys. Rev. Lett. **108**(21), 218703 (2012).

[41]E. T. Bullmore and O. Sporns, "Complex brain networks: Graph theoretical analysis of structural and functional systems," Nat. Rev. Neurosci. **10**(3), 186–198 (2009).

[42]W. Z. Kong, W. C. Lin, F. Babiloni, S. Q. Hu, and G. Borghini, "Investigating driver fatigue versus alertness using the granger causality network," Sensors **15**(8), 19181–19198 (2015).

[43]S. Supriya, S. Siuly, H. Wang, J. L. Cao, and Y. C. Zhang, "Weighted visibility graph with complex network features in the detection of epilepsy," IEEE Access **4**, 6554–6566 (2016).

[44]L. Lacasa, V. Nicosia, and V. Latora, "Network structure of multivariate time series," Sci. Rep. **5**, 15508 (2015).

[45]L. Lacasa and R. Toral, "Description of stochastic and chaotic series using visibility graphs," Phys. Rev. E **82**(3), 036120 (2010).

[46]Z. K. Gao, Q. Cai, Y. X. Yang, W. D. Dang, and S. S. Zhang, "Multiscale limited penetrable horizontal visibility graph for analyzing nonlinear time series," Sci. Rep. **6**, 35622 (2016).
[47]Q. Cai, Z. K. Gao, Y. X. Yang, W. D. Dang, and C. Grebogi, "Multiplex limited penetrable horizontal visibility graph from EEG signals for driver fatigue detection," Int. J. Neural Syst. **29**(5), 1850057 (2019).
[48]U. Herwig, P. Satrapi, and C. Schonfeldt-Lecuona, "Using the international 10-20 EEG system for positioning of transcranial magnetic stimulation," Brain Topogr. **16**(2), 95–99 (2003).
[49]M. Kleiner, "Visual stimulus timing precision in psychtoolbox-3: Tests, pitfalls and solutions," Perception **39**(S), 189 (2010).
[50]S. Ajami, A. Mahnam, and V. Abootalebi, "An adaptive SSVEP-based brain-computer interface to compensate fatigue-induced decline of performance in practical application," IEEE Trans. Neural. Syst. Rehabil. Eng. **26**(11), 2200–2209 (2018).
[51]S. P. Heinrich, "Some thoughts on the interpretation of steady-state evoked potentials," Doc. Ophthalmol. **120**(3), 205–214 (2010).
[52]D. H. Zhu, J. Bieger, G. Garcia Molina, and R. M. Aarts, "A survey of stimulation methods used in SSVEP-based BCIs," Comput. Intell. Neurosci. **2010**, 12 (2010).
[53]E. M. A. Smets, B. Garssen, B. Bonke, and J. C. J. M. De Haes, "The multidimensional fatigue inventory (MFI) psychometric qualities of an instrument to assess fatigue," J. Psychosom. Res. **39**(3), 315–325 (1995).
[54]A. Delorme and S. Makeig, "EEGLAB: An open source toolbox for analysis of single-trial EEG dynamics including independent component analysis," J. Neurosci. Methods **134**(1), 9–21 (2004).
[55]T. P. Jung, S. Makeig, C. Humphries, T. W. Lee, M. J. McKeown, V. Iragui, and T. J. Sejnowski, "Removing electroencephalographic artifacts by blind source separation," Psychophysiology **37**(2), 163–178 (2000).
[56]C. S. Herrmann, "Human EEG responses to 1–100 Hz flicker: Resonance phenomena in visual cortex and their potential correlation to cognitive phenomena," Exp. Brain Res. **137**(3-4), 346–353 (2001).
[57]S. Zeki, J. D. Watson, C. J. Lueck, K. J. Friston, C. Kennard, and R. S. Frackowiak, "A direct demonstration of functional specialization in human visual cortex," J. Neurosci. **11**(3), 641–649 (1991).
[58]D. R. Hardoon, S. Szedmak, and J. Shawe-Taylor, "Canonical correlation analysis: An overview with application to learning methods," Neural Comput. **16**(12), 2639–2664 (2004).
[59]Z. L. Lin, C. S. Zhang, W. Wu, and X. R. Gao, "Frequency recognition based on canonical correlation analysis for SSVEP-based BCIs," IEEE Trans. Biomed. Eng. **53**(12), 2610–2614 (2006).
[60]M. A. Hearst, "Support vector machines," IEEE Intell. Syst. App. **13**(4), 18–21 (1998).
[61]A. Subasi and M. I. Gursoy, "EEG signal classification using PCA, ICA, LDA and support vector machines," Expert. Syst. Appl. **37**(12), 8659–8666 (2010).
[62]M. R. Xia, J. H. Wang, and Y. He, "Brainnet viewer: A network visualization tool for human brain connectomics," PLoS One **8**(7), e68910 (2013).
[63]C. E. Ginestet, T. E. Nichols, E. T. Bullmore, and A. Simmons, "Brain network analysis: Separating cost from topology using cost-integration," PLoS One **6**(7), e21570 (2011).
[64]M. Rubinov and O. Sporns, "Complex network measures of brain connectivity: Uses and interpretations," Neuroimage **52**(3), 1059–1069 (2010).
[65]M. G. Kitzbichler, R. N. A. Henson, M. L. Smith, P. J. Nathan, and E. T. Bullmore, "Cognitive effort drives workspace configuration of human brain functional networks," J. Neurosci. **31**(22), 8259–8270 (2011).
[66]C. Zhang, F. Y. Cong, and H. Wang, "Driver fatigue analysis based on binary brain networks," ICIST **2017**, 485–489 (2017).
[67]R. Ferri, F. Rundo, O. Bruni, M. G. Terzano, and C. J. Stam, "Small-world network organization of functional connectivity of EEG slow-wave activity during sleep," Clin. Neurophysiol. **118**(2), 449–456 (2007).